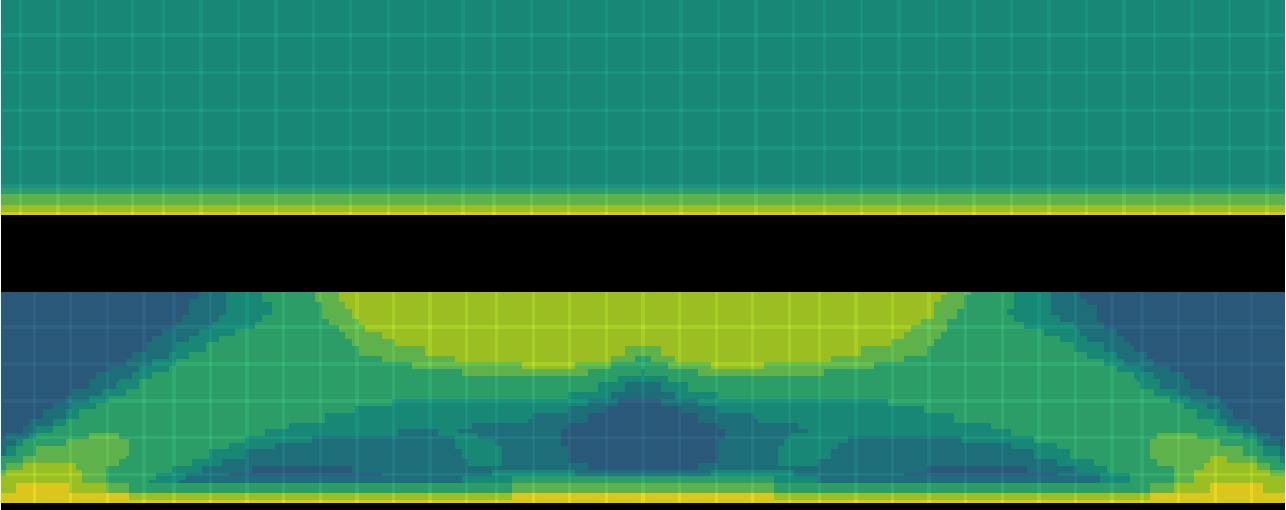

Optimal designs with topology optimisation

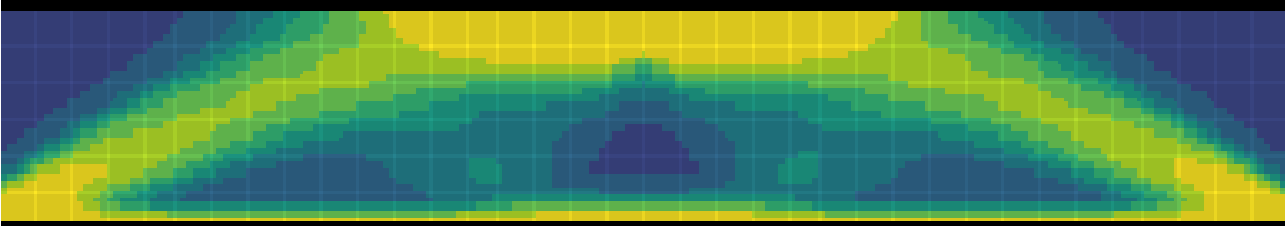

Literature report

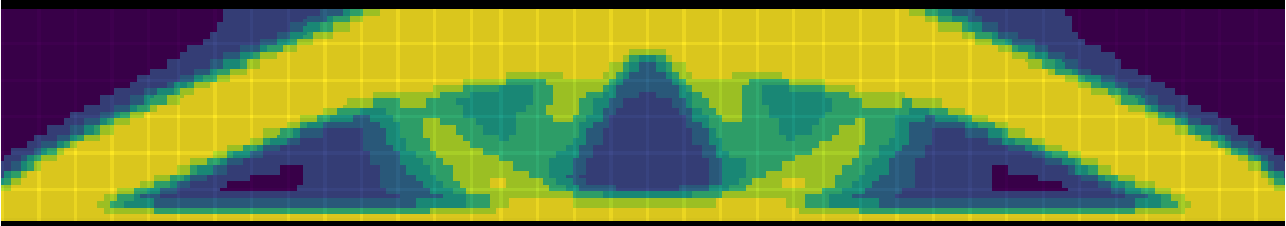

A. B. L. Frank

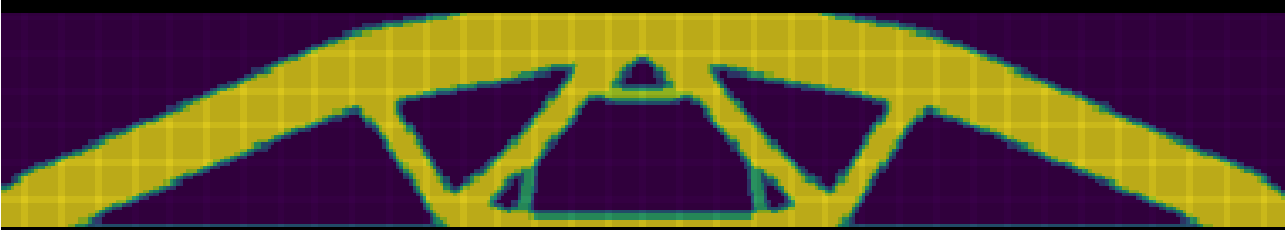

Optimal designs with topology optimisation

by

A.B.L. FRANK

Mid term review literature report
to obtain permission to conduct the proposed research
for the Master of Science
at the Delft University of Technology,
to be presented privately on November 24, 2021 at 14:00.

Student number: 4603443
Project duration: July 26, 2021 – November 24, 2021

Mid term review committee

Daily supervisor university
Dr. ir. D. den Ouden-van der Horst Delft University of Technology

Responsible professor
Prof. dr. ir. C.Vuik Delft University of Technology

This literature report is confidential and cannot be made public until November 24, 2021

An electronic version of this thesis is available at request:
A.B.L.Frank@student.tudelft.nl

TU Delft

PREFACE

It is custom to thank everyone in the preface. However, I leave that to the preface of the final report of my master thesis. Now, I would like to address that this master thesis project is conducted at Delft University of Technology in cooperation with Sioux Mathware in Eindhoven. At Sioux João Pereira Machado and Timo van Opstal oversee the project and provide any necessities. The graduation takes place at the department of numerical analysis of which Kees Vuik is the professor. Under the guidance of Dennis den Ouden-van der Horst I would like to contribute to the field of mathematics.
This literature report serves as an appetiser and the final report is the main course. Enjoy!

Abel Frank
Delft, November 29

CONTENTS

Preface **iii**

1 Introduction **1**
1.1 Field of interest . . . 1
1.2 Historical background . . . 2
1.3 Research problem . . . 4
1.4 Thesis objectives . . . 4
1.5 The reader's guide to the literature report . . . 5

2 Preliminaries **7**
2.1 The physical design . . . 7
2.1.1 Material properties . . . 7
2.1.2 Physical constraints . . . 8
2.2 Mathematical domain . . . 8

3 Problem derivation **11**
3.1 Linear elasticity . . . 11
3.1.1 Stiffness tensor . . . 12
3.2 The principle of minimum potential energy . . . 13
3.3 Minimum compliance problem . . . 14
3.4 Fundamental eigenfrequency maximisation problem . . . 15
3.5 The level-set method . . . 16
3.5.1 Properties of the level-set function . . . 16
3.6 Implementing the level-set method . . . 18
3.6.1 Level-set embedded minimum compliance problem . . . 19
3.6.2 Level-set embedded fundamental eigenfrequency maximisation problem . . . 19

4 Benchmark problems **21**
4.1 Comparative topology optimisation method . . . 21
4.2 MBB beam . . . 21
4.2.1 Numerical example MBB beam . . . 23
4.3 Cantilever . . . 23

4.3.1 Numerical example cantilever 24
4.4 Inverter 24
4.4.1 Numerical example inverter 25

5 Conclusive summary **27**

A Derivation of the equation of motion **29**

B Nomenclature **31**

CHAPTER 1

INTRODUCTION

1.1 Field of interest

Structures (e.g. bridges, beams and hinges) with optimal designs are becoming more significant in our society in which efficiency and sustainability are vital. Obtaining the most efficient design for complex structures is a delicate task of colossal (industrial) importance. Optimal designs lead to better performances and lighter structures and save design materials. A drawback of optimal designs is that they may be expensive or difficult to manufacture. Traditional design methods primarily deal with straightforward and basic geometries. This obviously puts a restriction on the complexity of the structures one might want to design and optimise.
Nowadays, fortunately, there are methods which do not have this problem. Three commonly used methods are size, shape and topology optimisation. While size and shape optimisation methods require close-to-optimal initial designs, topology optimisation does not. In topology optimisation an objective function is minimised (or maximised) under physical and geometrical constraints with the material distribution as a problem variable. In other words, the aim of topology optimisation is to find the optimal design under an objective and adhering a number of constraints.
A major part of this thesis focuses on a particular topology optimisation problem, namely the minimum compliance problem. The objective is to find a design for which the compliance is minimal under a number of constraints. In the context of linear elasticity the compliance is equivalent to the strain energy. This energy dictates the stiffness of a structure in the following way: if the strain energy is minimal, the stiffness of the design is maximal.
Although topology optimisation yields many advantages in comparison to older methods, solving the affiliated minimum compliance problem poses some obstacles. Finding analytical solutions turns out to be a tedious task and in most cases they do not exist. Even solving the minimum compliance problem numerically presents us with specific issues. Three common numerical problems are the formation of checkerboards, mesh dependency and local minima, which amongst others will be discussed in Section 1.2.

In light of these numerical problems, level-set methods (LSM) have been proposed to circumvent them. Moreover, level-set based topology optimisation methods yield a beneficial treatment of changes in the topology during simulation. In level-set methods, the design domain is represented implicitly by a level-set function, of which the zero interface describes the surface of this domain.
In addition to level-set based topology optimisation, eigenvalue optimisation has gained some interest during the beginning of this millennium. In many regards the eigenvalue topology optimisation problem is the same as the minimum compliance problem. However, the main difference is the objective function. There are different types of eigenfrequency optimisation. In this thesis we want to find the optimal design such that the first (i.e. smallest) eigenfrequency is maximised. The reason one wants to maximise this eigenfrequency, is to minimise the vibrations of a structure when a certain force is applied. Besides the minimum compliance problem, the fundamental eigenfrequency maximisation problem is treated thoroughly.

1.2 Historical background

In the year 1988 two very important mathematical papers were published. The topic of each paper plays a major role in this thesis. Bendsøe and Kikuchi [7] are the founding fathers of topology optimisation and Sethian and Osher [18] the architects of the level-set method.
In 1988 Bendsøe and Kikuchi introduced a method which generates optimal topologies utilising the homogenisation method (for more information on the homogenisation method for topology optimisation, see [34], [1]). In their paper the foundation for topology optimisation was laid. Since then, numerous topology optimisation approaches have been developed. The basis of these approaches, however, is the same and gives answer to the fundamental question of topology optimisation: where to place material in a prescribed domain for the best structural performance?
For a broader review of the field of topology optimisation see the 2014 survey of Deaton and Grandhi [10]. For a comparison of the different topology optimisation methods see the comparative review of Sigmund and Maute [30].
A branch of topology optimisation that does not get a lot of attention, but is worth exploring, is eigenvalue topology optimisation. Tenek and Hagiwara were the first to compute structures for which the first eigenfrequency was maximised using homogenisation and mathematical programming [36]. Another notable work in this field of research is the 2000 paper of Pedersen [20].
Naturally, problems occur when solving a topology optimisation problem. The 0-1 topology optimisation problem, for example, lacks analytical solutions in general [31], [30]. However, there are some cases for which an analytical solution is found [22], [23], [12], [13], [14]. Furthermore, there are numerical problems. In their 1998 review article [31] Sigmund and Petersson indicate three common numerical problems that occur in topology optimisation. First, there is the formation of checkerboards. This is the construction of alternating void and solid elements ordered in a checkerboard structure caused by the non-convergence of finite-element solutions. Second, we have mesh dependency. This refers to the problem that for different mesh-sizes or discretisations one does not obtain qualitatively the same solution. Third, there is the

existence of local minima. This means that for the same discretisation one obtains different solutions if algorithmic parameters are altered, e.g., different starting designs. This is caused by the numerical optimisation procedures of the algorithm.
Since 1988 a number of different approaches has been developed as Sigmund and Maute point out in their review article [30]. These include density, level-set, topological derivative, phase field and evolutionary approaches. A thorough comparison of these different approaches and other literature reference can be found in the same review article.
As this thesis focuses on the level-set approach, it is important to understand what the level-set method is. In 1988 Sethian and Osher published a paper about capturing fronts propagating with curvature-dependent speed [18]. Later it was named the level-set method and is thoroughly described in the book of Osher and Fedkiw [17]. This method describes how one keeps track of a level-set (in most cases the zero level contour) of a function. This function is called the level-set function and the contour is also referred to as the interface, as it separates two regions.
In 2000 the level-set method was applied in topology optimisation for the first time by Sethian and Wiegmann [26]. Since then, various level-set based topology optimisation methods have arisen. These can be classified, for example, by the approach for updating the level-set field in the optimisation process and the method for discretising the level-set function. In their review article Van Dijk et al. pay attention to theses different approaches and discuss the level-set approach in general [37].
The level-set method for topology optimisation was introduced because of the special properties of the level-set function. The function is used to implicitly define the interfaces between materials by iso-contours. This allows for a neat description of the interfaces. Some notable works in the field of level-set topology optimisation are that of Noël et al. [16] who use hierarchical B-splines to disretise the state variable fields and level-set function, Yaji et al. [39] who embed the reinitialisation in the time evolution equation utilising a convected level-set method and Allaire and Jouve [3] who adapted the method for stress minimisation.
In the field of level-set topology optimisation, some research has been done in the area of eigenfrequency optimisation by Osher and Santosa [19], Allaire and Jouve [2], De Gournay [9] and Yamada et al. [40].
The reason we choose a level-set based topology optimisation over other approaches is because it holds many advantages and it is a relatively new approach. The main advantage is that the interface is clearly and smoothly described implicitly by the level-set function. In addition, Allaire et al. state a number of benefits for the level-set approach in their 2004 paper [5]. The method permits radical topological changes during the optimisation process, the CPU time is reasonable and it can handle general mechanical models (including nonlinear ones) and objective functionals. In the aforemention comparative review paper of Sigmund and Maute [30] the level-set approach is also reviewed. They remark that the level-set method is “well suited for capturing stochastic shape variations for robust design optimization”. In the review article of Van Dijk et al. it is also noted that a level-set based topology optimisation treats topological changes conveniently, unlike explicit boundary description methods. This means that during the optimisation process holes can fuse together and new connections can be made in the design.
Unfortunately, there are drawbacks to a level-set approach for topology optimisation.

A huge deficiency in the conventional level-set approach is that it does not allow the nucleation of holes. This is noted by Allaire et al. and techniques to circumvent this are briefly outlined. This lack of hole nucleation makes the optimal design heavily dependent on the initial design as stated in plentiful works [39], [5], [37], [30]. Furthermore, similar to the traditional topology optimisation method, the level-set based method suffers from local minima according to Van Dijk et al. [37] and Allaire and Jouve [2]. Luckily, the majority of these obstacles has been dealt with.
However, there is also a non-numerical problem in topology optimisation. This will be part of the research problem and is discussed in the next section.

1.3 Research problem

The use of standard benchmark problems for topology optimisation methods is briefly addressed in the 2013 comparative review article of Sigmund and Maute [30]. While the MBB beam and cantilever are typical benchmark problems in literature, there is a lack of challenging standard test cases. Moreover, they mention a specifically "challenging but still simple to implement compliant mechanism benchmark": the inverter. It was first proposed by Sigmund in 1997 [27] and used as a 'standard' benchmark problem in later works of him and co-writers [28], [29]. In Section 4.4 the inverter benchmark problem will be thoroughly described.
Sigmund and Maute recommend in their review article that the inverter example should be chosen as a standard benchmark problem in future works regarding topology optimisation and in particular level-set based topology optimisation. The heavy influence of the initial design is a substantial burden for boundary control methods (e.g. level-set methods).
Another problem Sioux wishes to take on concerns eigenfrequency topology optimisation using a level-set method. They want an algorithm which maximises the fundamental eigenfrequency to reduce vibrations and increase the overall precision. Moreover, there is 'a lack of knowledge' in this field of research. Though stated as a "fundamental engineering design problem" by Deaton and Grandhi [10], there only is a modest amount of papers dedicated to this problem.

1.4 Thesis objectives

The first step of this thesis is to find out how a level-set embedded minimum compliance problem can be solved numerically. This means developing a topology optimisation algorithm based on the level-set method that is able to interact with a finite-element model and using it to find optimal designs. In view of this we set the following objectives:

- Derive a level-set embedded minimum compliance problem.
- Solve this problem numerically, which leads to an algorithm.
- Compare the results of this algorithm to known benchmarks: cantilever, MBB beam and inverter.

At the hand of these objectives we want to contribute to the solution for standardised benchmark problems.
Once the these objectives have been accomplished, we move on to the eigenfrequency problem. In respect to this problem we have the following problems:

- Derive a level-set embedded maximum fundamental eigenfrequency problem.
- Solve this problem numerically, which leads to an algorithm.
- Compare the results of this algorithm to known benchmarks.

The aim of these objectives is to make a contribution to the small-scaled field of level-set eigenvalue topology optimisation.

1.5 The reader's guide to the literature report

Now that a background of the main topic has been presented and the research problem of the thesis along with the corresponding objectives has been established, a concise overview of the outline of this literature report is provided.

Chapter 2 (Preliminaries)
Essential physical and material constraints as well clarifying mathematical notations are treated in this chapter.

Chapter 3 (Problem derivation)
Some elemental definitions of linear elasticity along with the principle of minimum potential energy are introduced at first. The main topic of this chapter is the derivation and formulation of the minimum compliance problem. In addition, the eigenfrequency maximisation topology optimisation problem is posed. Finally, the level-set method is presented and incorporated into both problems.

Chapter 4 (Benchmark problems)
Three benchmark problems regarding the minimum compliance problem are introduced and discussed thoroughly. Besides this, a topology optimisation method is briefly addressed and used to show some results of these benchmarks.

Chapter 5 (Conclusive summary)
The literature report is concluded with a concise summary and ends with a suggestion for the approach of the research problem.

CHAPTER 2

PRELIMINARIES

The physical and mathematical framework in which the problem of this thesis is presented is treated in this chapter. It begins with the physical aspects of the design material. Those aspects are then translated into a mathematical model.

2.1 The physical design

First and foremost, it must be noted that all physical designs are three-dimensional. However, as will be stated later, the mathematical problem can be two-dimensional as well. This is due to the fact that a two-dimensional mathematical shapes can be constructed as three-dimensional structures. In engineering this procedure is known as extrusion.
To start off, it is important to specify the properties we want our material to have.

2.1.1 Material properties

The material that will be used for the design is isotropic and homogeneous. A material is said to be isotropic if its properties are the same in all directions. Homogeneous means that a material has the same properties everywhere in the domain.
In Table 2.1 the parameter values of the design material are given. In this case the material is steel. These values are used in all codes and benchmark test cases.

Notation	**Definition**	**Value in SI units**
ρ	Density	$7.750\,\mathrm{kg}\cdot\mathrm{m}^{-3}$
E	Young's modulus	$190\cdot 10^{9}\,\mathrm{Pa}$
ν	Poisson ratio	0.28

Table 2.1: *Table of the parameter values of steel.*

2.1.2 Physical constraints

Naturally, the design does have a number of physical constraints. One of the most important constraints we pose on the design is a volume limit. This limit is defined as $V_{\max}$ and is a volume fraction. That is, it denotes a fraction of the total volume available to construct the design.
An essential element of designing is design constraints. These design constraints can be translated into physical constraints. Two of these are material constraints and two mechanical constraints. The material constraints dictate in which regions material must be present and in which no material is allowed.
The first mechanical constraint relates to the boundary conditions. The second states that the design structure must be connected. To be more specific we want the design structure to be path connected. In the next section these constraints are explained in more detail and expressed in mathematical terms.

2.2 Mathematical domain

It is imperative to define the mathematical domain in which we work. This can be either $\mathbb{R}^2$ or $\mathbb{R}^3$ in the case of topology optimisation. For the sake of generality, however, we shall refer to $\mathbb{R}^d$ where d is the dimension of the space. The domain we focus on is defined as *the reference domain* Ω. This domain is a subset of whole domain, i.e., $\Omega \subseteq \mathbb{R}^d$. We refer to the design material/structure as *the design domain* and assign it the letter D. This design domain is always 'inside' the reference domain, i.e., $D \subseteq \Omega$. The boundary of the design domain ∂D is denoted by Γ. All space within the reference domain that is not material is called the void.
To make a clear distinction between a volume integral (area or length integral in $\mathbb{R}^2$ or $\mathbb{R}$, respectively) and a surface integral (line or point integral in $\mathbb{R}^2$ or $\mathbb{R}$, respectively) we also use the capital Greek letters omega and gamma to denote these integrals, respectively. So, a volume integral has the differential $\mathrm{d}\Omega$ and a surface integral $\mathrm{d}\Gamma$.
Promptly, more specific information about the reference and design domain is given.

Reference domain

The reference domain can have any fixed form. So, it does not necessarily need to be a square (or cube) or circle (or sphere). Due to this definition of the reference domain, we give the design domain a predefined space in which we want it to be optimised. It also puts a limit on the available space for the design domain. That is to say, the aforementioned volume fraction $V_{\max}$ is a fraction of the volume of the reference domain. Thus, the reference domain is the space in which the design can attain its optimal structure. A pleasant fortuity is that we can create holes in the reference domain which serve as regions where no material is allowed. Furthermore, the boundary of the reference domain, $\partial\Omega$, is significant too, as it is needed to define the boundary conditions of the level-set function. However, this will be accounted for after the level-set method is introduced and implemented in the minimum compliance problem (see Section 3.6).

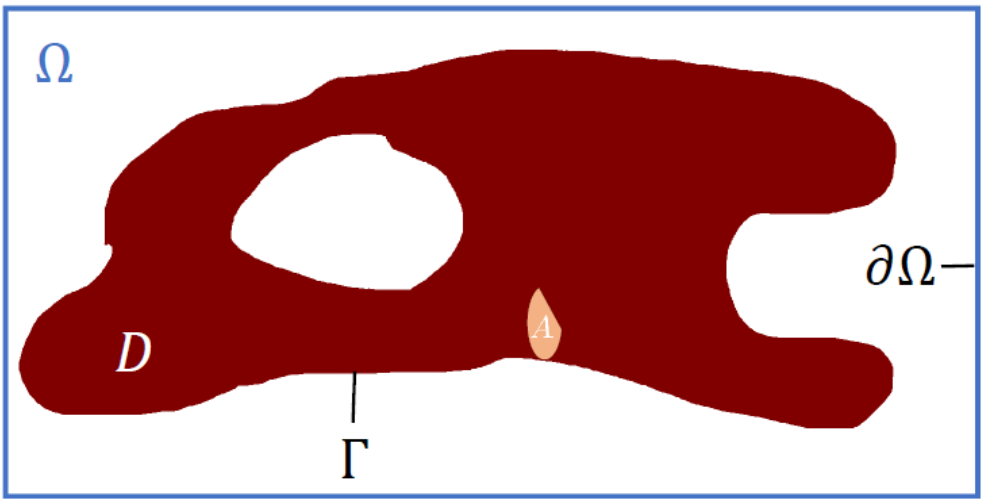

Figure 2.1: *Two-dimensional visualisation of the mathematical domain. Ω is the reference domain and $\partial\Omega$ its boundary. The design domain is D and Γ its boundary. Material is always present in A*

Design domain

The objective of topology optimisation is to find the optimal design. Therefore, we must be clear on what the design domain D is. It is crucial to keep in mind that the design domain will be updated during the optimisation process. This means that we start with an initial design and end up with an optimal one.
The design domain D is the set of coordinates where material is present. It is contained in the reference domain and cannot exist outside of it. Due to possible design constraints we allow the initial design domain to have predefined holes. Moreover, it is even possible that new holes are created as a consequence of the topology optimisation. Another crucial property of the design domain is that it must always be path connected, even after topology optimisation is applied. That is, one can follow a path from an arbitrary point in D to any other point in D, without crossing its boundary. We must also take into account that there may be parts of the design domain where material must be present. Therefor we define the domain $A \subseteq D$. That it is, A is the subset of D where there is always material. A simple visualisation of all this is given in Figure 2.1.

Boundary conditions on Γ

In this thesis only two types of boundary conditions are considered: Dirichlet boundary conditions (named after Peter Gustav Lejeune Dirichlet) and Neumann boundary conditions (named after Carl Neumann). Therefore we define Γ_{D}, the part of the boundary which has Dirichlet boundary conditions, and Γ_{N}, the part which has Neumann boundary conditions, such that $\Gamma = \Gamma_{\mathrm{D}} \cup \Gamma_{\mathrm{N}}$. These boundary conditions apply to the displacement $\mathbf{u}$ (which is explained in Chapter 3). Moreover, some parts of

the boundary can have both boundary conditions. However, a single displacement component can only have one boundary condition. Dirichlet boundary conditions are denoted with $\mathbf{u}_0$. If no explicit boundary condition is stated for a certain part of the boundary it is assumed to have a homogeneous Neumann boundary condition.

Place-dependency of parameters and constants

Because we make a clear difference between material and void, the parameters and constants we encounter are place-dependent in a certain way. Inside the design domain, i.e., in the material, the parameters and constants exist. As the material is isotropic and homogeneous the parameters and constants remain the same everywhere inside the design domain. On the other hand, in the void, those parameters and constants do not exist. So, the parameters and constants could be expressed with the use of an indicator function, but that would only be necessary in computational cases. Thus, we will refrain from denoting parameters and constants as functions of place.

CHAPTER 3

PROBLEM DERIVATION

In this chapter we compose the topology optimisation problem after a brief introduction to linear elasticity and the principle of minimum potential energy in physics. Then, the minimum compliance problem is derived and the fundamental eigenfrequency maximisation problem is posed. Finally, we implement the level-set method into both problems. First, we look at the physics of linear elasticity.

3.1 Linear elasticity

Elasticity involves a change of shape, so we define the displacement vector $\mathbf{u}(\mathbf{x})$ as a function of the location $\mathbf{x} \in \mathbb{R}^d$. As stated by Sadd [25] the (Cauchy) strain consists of *normal strain*, which is "the change in length per unit length of fibers oriented in the normal direction", and *shear strain*, which is "the change in angle between two originally orthogonal directions in the continuum material'. According to Sadd [25] there is a relation between the displacement and the strain, which is called the *strain-displacement relation*

$$\underline{\underline{\varepsilon}}(\mathbf{u}) := \frac{1}{2}\left(\nabla\mathbf{u} + (\nabla\mathbf{u})^T\right), \quad \varepsilon_{ij} = \frac{1}{2}\left(\frac{\partial u_i}{\partial x_j} + \frac{\partial u_j}{\partial x_i}\right). \tag{3.1}$$

Note that $\underline{\underline{\varepsilon}}(\mathbf{u})$ is a symmetric by definition. Be aware of the fact that the strain-displacement relation is linearised. Ergo linear elasticity. For more information regarding the theory of nonlinear elasticity see Antman's book [6] (in the context of mathematics) or Rushchitsky's book [24] (in the context of physics). If one is interested in nonlinear elasticity in relation to topology optimisation, the 2004 paper of Allaire et al. [5] is recommended.
Another very important physical quantity is stress. In order to express the stress in terms of the strain we utilise the generalised Hooke's law (named after Robert Hooke) for linear isotropic elastic materials [32]:

$$\underline{\underline{\varepsilon}} = \frac{1}{E}\left[(1+\nu)\underline{\underline{\sigma}} - \nu\mathrm{tr}(\underline{\underline{\sigma}})I\right], \tag{3.2}$$

where E is Young's modulus, ν the Poisson ratio (named after Thomas Young and Siméon Poisson, respectively), $\underline{\underline{\sigma}}$ the stress tensor and I the identity matrix. In index notation this becomes $\varepsilon_{ij} = \frac{1}{E}\left[(1+\nu)\sigma_{ij} - \nu\delta_{ij}\sigma_{kk}\right]$, where $\sigma_{kk} = \sum_{i=1}^{d}\sigma_{ii}$ and δ_{ij} is the Kronecker delta function (named after Leopold Kronecker). Remark that

$$\begin{aligned}\varepsilon_{kk} &= \frac{1}{E}\left[(1+\nu)\sigma_{11} - \nu\sigma_{kk} + (1+\nu)\sigma_{22} - \nu\sigma_{kk} + (1+\nu)\sigma_{33} - \nu\sigma_{kk}\right] \\ &= \frac{1}{E}\left[(1+\nu)\sigma_{kk} - 3\nu\sigma_{kk}\right] = \frac{1-2\nu}{E}\sigma_{kk}.\end{aligned}$$

This gives $\sigma_{kk} = \frac{E}{1-2\nu}\varepsilon_{kk}$. Now we can express the stress tensor in terms of the linear strain tensor.

$$\sigma_{ij} = \frac{E}{1+\nu}\varepsilon_{ij} + \frac{\nu E}{(1+\nu)(1-2\nu)}\delta_{ij}\varepsilon_{kk}.$$

If we introduce the Lamé constants, $\lambda = \frac{\nu E}{(1+\nu)(1-2\nu)}$ and $\mu = \frac{E}{2(1+\nu)}$ (named after Gabriel Lamé), we can give the constitutive equation for isotropic materials (Hooke's law) as described in [32].

$$\underline{\underline{\sigma}}(\mathbf{u}) = 2\mu\underline{\underline{\varepsilon}}(\mathbf{u}) + \lambda\mathrm{tr}(\underline{\underline{\varepsilon}}(\mathbf{u}))I. \tag{3.3}$$

It should be mentioned that μ is also known as the shear modulus in the context of elasticity.

3.1.1 Stiffness tensor

As we are dealing with linear elasticity, the stress components are assumed to be linear functions of the strain components. So, following Equation (3.3) we can express the stress as

$$\sigma_{ij}(\mathbf{u}) = E_{ijkl}\varepsilon_{kl}(\mathbf{u}), \quad \text{with} \quad E_{ijkl} = \mu(\delta_{ik}\delta_{jl} + \delta_{il}\delta_{jk}) + \lambda\delta_{ij}\delta_{kl}. \tag{3.4}$$

The term E_{ijkl} is called the stiffness tensor and for an isotropic homogeneous material has the following symmetry properties:

$$E_{ijkl} = E_{jikl}, \qquad E_{ijkl} = E_{ijlk}, \qquad E_{ijkl} = E_{klij}. \tag{3.5}$$

The first two symmetries are a consequence of the symmetry of the strain in Equation (3.1). Due to the third symmetry we can define the following symmetric bilinear function in Einstein notation (named after Albert Einstein):

$$a(\mathbf{u},\mathbf{v}) := \int_D E_{ijkl}\varepsilon_{kl}(\mathbf{u})\varepsilon_{ij}(\mathbf{v})\,\mathrm{d}\Omega, \tag{3.6}$$

where D is the aforementioned design domain. Definition (3.6) is loosely based on an inner product introduced by Eremeyev and Lebedev in [11]. Later, we will see that Definition (3.6) is the energy bilinear form as described by Bendsøe and Sigmund in [8] and used in the formulation of the minimum compliance problem. Using the

stiffness tensor expression of the stress (see Equation (3.4)), Definition (3.6) can be written as

$$a(\mathbf{u}, \mathbf{v}) = \int_D \underline{\underline{\sigma}}(\mathbf{u}) : \underline{\underline{\varepsilon}}(\mathbf{v}) \, \mathrm{d}\Omega. \tag{3.7}$$

Here the Frobenius inner product (named after Ferdinand Georg Frobenius) is used. The Frobenius inner product for two complex-valued $n \times m$ matrices A and B is defined as follows:

$$A : B := \langle A, B \rangle_{\mathrm{F}} = \sum_{i,j} \overline{A_{ij}} B_{ij}, \tag{3.8}$$

where the overline denotes the complex conjugate. It follows from its definition that the Frobenius inner product is sesquilinear.

3.2 The principle of minimum potential energy

From the principle of minimum potential energy we can derive the weak form of linear elasticity, which is called the *the principle of virtual work* in stress analysis. The minimum potential energy problem of an elastic body, based on [32] and [11], is defined as

$$\begin{cases} \text{Find } \mathbf{u} \in U \text{ such that } P(\mathbf{u}) \leq P(\mathbf{v}) \ \forall \mathbf{v} \in U, \text{ for} \\ P(\mathbf{u}) = \frac{1}{2} \int_D \underline{\underline{\sigma}}(\mathbf{u}) : \underline{\underline{\varepsilon}}(\mathbf{u}) \, \mathrm{d}\Omega - \int_\Gamma \mathbf{t} \cdot \mathbf{u} \, \mathrm{d}\Gamma - \int_D \mathbf{f} \cdot \mathbf{u} \, \mathrm{d}\Omega, \end{cases} \tag{3.9}$$

where $\mathbf{t}$ is the (external) traction, $\mathbf{f}$ the (internal) body forces and U the set of all accessible displacements. Traction forces only act on the boundary of the design domain. Traction can be seen as the force which makes an object move over a surface by overcoming all resisting forces. In our case we regard externally applied traction forces. Body force is a force that acts on the entire design domain, that is, it acts throughout the volume of a structure. Examples of body forces are gravity and magnetism.

Now, we want to find weak extrema of the functional $P(\mathbf{u})$ which denotes the *total strain energy for an elastic body*. Therefore we look at the calculus of variations. This tells us that a necessary condition for finding weak extrema for Problem (3.9) is the Euler-Lagrange equation

$$\frac{\mathrm{d}}{\mathrm{d}\beta} P(\mathbf{u} + \beta \mathbf{v}) \Big|_{\beta=0} = 0 \tag{3.10}$$

for any fixed virtual displacement $\mathbf{v} \in U_0 := \{\mathbf{w} \in U : \mathbf{w} = \mathbf{0} \text{ on } \Gamma_{\mathrm{D}}\}$ and $\mathbf{u}$ the optimal solution of Problem (3.9). Here, U_0 denotes the set of admissible displacements with homogeneous boundary conditions.

Before we express the Euler-Lagrange equation, note that the functional $P(\mathbf{u})$ can be expressed with the aforementioned symmetric bilinear function a, see Definition (3.6).

$$P(\mathbf{u}) = \frac{1}{2} a(\mathbf{u}, \mathbf{u}) - \int_\Gamma \mathbf{t} \cdot \mathbf{u} \, \mathrm{d}\Gamma - \int_D \mathbf{f} \cdot \mathbf{u} \, \mathrm{d}\Omega.$$

Using this expression for the functional, we first look at $P(\mathbf{u}+\beta\mathbf{v})$ and express it using the symmetric and bilinear properties of $a(\mathbf{u},\mathbf{v})$.

$$P(\mathbf{u}+\beta\mathbf{v}) = \frac{1}{2}a(\mathbf{u},\mathbf{u})+\beta a(\mathbf{u},\mathbf{v})+\frac{1}{2}\beta^2 a(\mathbf{v},\mathbf{v})-\int_\Gamma \mathbf{t}\cdot\mathbf{u}\ \mathrm{d}\Gamma-\beta\int_\Gamma \mathbf{t}\cdot\mathbf{v}\ \mathrm{d}\Gamma-\int_D \mathbf{f}\cdot\mathbf{u}\ \mathrm{d}\Omega-\beta\int_D \mathbf{f}\cdot\mathbf{v}\ \mathrm{d}\Omega.$$

We take the derivative with respect to β.

$$\frac{\mathrm{d}}{\mathrm{d}\beta}P(\mathbf{u}+\beta\mathbf{v}) = a(\mathbf{u},\mathbf{v}) + \beta a(\mathbf{v},\mathbf{v}) - \int_\Gamma \mathbf{t}\cdot\mathbf{v}\ \mathrm{d}\Gamma - \int_D \mathbf{f}\cdot\mathbf{v}\ \mathrm{d}\Omega.$$

Now we set $\beta = 0$ and equate the result to zero.

$$a(\mathbf{u},\mathbf{v}) - \int_\Gamma \mathbf{t}\cdot\mathbf{v}\ \mathrm{d}\Gamma - \int_D \mathbf{f}\cdot\mathbf{v}\ \mathrm{d}\Omega = 0.$$

So, the weak form of linear elasticity is

$$\int_D \underline{\underline{\sigma}}(\mathbf{u}) : \underline{\underline{\varepsilon}}(\mathbf{v})\,\mathrm{d}\Omega = \int_D \mathbf{f}\cdot\mathbf{v}\,\mathrm{d}\Omega + \int_\Gamma \mathbf{t}\cdot\mathbf{v}\,\mathrm{d}\Gamma \qquad \forall\mathbf{v}\in U_0. \tag{3.11}$$

From Equation (3.11) the equation of motion for elastostatics can be derived. For this derivation look at Appendix A.

3.3 Minimum compliance problem

As mentioned before, the integral in Definition (3.6) is used in the minimum compliance problem as the internal virtual work. The integral on the right-hand side of Equation (3.11) is called the *load linear form* [8]. We define the functional

$$l(\mathbf{u}) := \int_D \mathbf{f}\cdot\mathbf{u}\ \mathrm{d}\Omega + \int_\Gamma \mathbf{t}\cdot\mathbf{u}\ \mathrm{d}\Gamma. \tag{3.12}$$

The way we define the minimum compliance problem is roughly based on the same problem defined by Bendsøe and Sigmund in their book [8].

$$\begin{cases} \min\limits_D & a(\mathbf{u},\mathbf{u}) \\ \text{s.t.} & a(\mathbf{u},\mathbf{v}) = l(\mathbf{v}), \quad \forall\mathbf{v}\in U_0, \\ & \mathbf{u}\big|_{\Gamma_\mathrm{D}} = \mathbf{u}_0, \\ & D \text{ is path connected}, \\ & \int\limits_D 1\,\mathrm{d}\Omega \le V_{\max}\int\limits_\Omega 1\,\mathrm{d}\Omega. \end{cases} \tag{3.13}$$

Here D and Γ_D are as described in Section 2.2.
The objective of our problem is to find the optimal design domain for which the compliance is minimal. This is equivalent to minimising the strain energy ($\frac{1}{2}a(\mathbf{u},\mathbf{u})$)

over D. Note that this is the same as minimising $a(\mathbf{u}, \mathbf{u})$ over D. What is more, we need to minimise over D and not over $\mathbf{u}$. That is because $\mathbf{u}$ is a function of the design domain D for $\mathbf{u}$ is determined by the principle of minimum potential energy which depends on D. Furthermore, we have the physical constraint regarding that principle, a boundary condition and the volume constraint, in that order. Because the eigenfrequency topology optimisation problem is based on comparable physical constraints, we introduce it forthwith.

3.4 Fundamental eigenfrequency maximisation problem

In the context of eigenvalues, it is common to order eigenvalues from smallest to biggest, i.e., $\eta_1 \leq \eta_2 \leq ... \leq \eta_n$. So, the first eigenvalue, η_1, is the smallest and also referred to as the *fundamental eigenvalue*. In the context of vibrations we have eigenfrequencies, i.e. the square root of the eigenvalue. Then, [15] uses the following equation as the weak form of the equation of motion for the k-th eigenfrequency:

$$a\left(\mathbf{u}^{(k)}, \mathbf{v}\right) = \omega_k^2 b\left(\mathbf{u}^{(k)}, \mathbf{v}\right), \quad \forall \mathbf{v} \in U_0, \tag{3.14}$$

where

$$b(\mathbf{u}, \mathbf{v}) := \int_D \rho \mathbf{u} \cdot \mathbf{v} \, \mathrm{d}\Omega. \tag{3.15}$$

The functional b is known as the *structural mass form*. Note that the term $l(\mathbf{v})$ is left out, because the body and traction forces are neglected for the eigenvalue problem. Furthermore, ω_k is the k-th eigenfrequency corresponding to the k-th eigenfunction $\mathbf{u}^{(k)}$. Our curiosity for the fundamental eigenfrequency is connected to the phenomenon known as resonance. If resonance occurs, the structure would be vibrating heavily and we want to prevent that. In nature lower frequencies are more common than higher frequencies. So, the first eigenfrequency is more susceptive to resonance than the other frequencies. To that end we want to maximise the fundamental eigenfrequency which can be expressed as the minimum value of the Rayleigh quotient (named after John William Strutt, 3rd Baron Rayleigh) according to Allaire and Jouve [2].

$$\omega_1^2 = \min_{\mathbf{v} \in U_0 \wedge \mathbf{v} \neq \mathbf{0}} \frac{a(\mathbf{v}, \mathbf{v})}{b(\mathbf{v}, \mathbf{v})}. \tag{3.16}$$

The fundamental eigenfrequency maximisation problem is defined as follows

$$\begin{cases} \max\limits_{D} & \omega_1^2 \\ \text{s.t.} & a\left(\mathbf{u}^{(1)}, \mathbf{v}\right) = \omega_1^2 b\left(\mathbf{u}^{(1)}, \mathbf{v}\right), \quad \forall \mathbf{v} \in U_0, \\ & \mathbf{u}^{(1)}\big|_{\Gamma_\mathrm{D}} = \mathbf{u}_0^{(1)}, \\ & \int\limits_D 1 \, \mathrm{d}\Omega \leq V_{\max} \int\limits_\Omega 1 \, \mathrm{d}\Omega. \end{cases} \tag{3.17}$$

Remark the resemblance to the minimum compliance problem, Problem (3.13). The main difference is obviously the objective, which is to find the optimal design for which

the fundamental eigenfrequency is maximal. Further, the first physical constraint is only considered for the first eigenfunction, i.e., the eigenfunction corresponding with the first eigenfrequency.
One of the goals of this thesis is to embed the level-set method into our minimum compliance problem, Problem (3.13), and fundamental eigenfrequency maximisation problem, Problem 3.17). Therefore, we digress and take a look at what a level-set function and the level-set method are.

3.5 The level-set method

The level-set method was introduced in 1988 by Sethian and Osher [18] in order to keep track of the motion of an arbitrary interface. The method involves using a level-set function

$$\begin{cases} \phi(\mathbf{x}) > 0 & \forall \mathbf{x} \in \Omega \setminus \overline{D}, \\ \phi(\mathbf{x}) = 0 & \forall \mathbf{x} \in \Gamma \cap \Omega, \\ \phi(\mathbf{x}) < 0 & \forall \mathbf{x} \in D \setminus \Gamma. \end{cases} \tag{3.18}$$

A visualisation of this scalar function is provided by Figure 3.1.

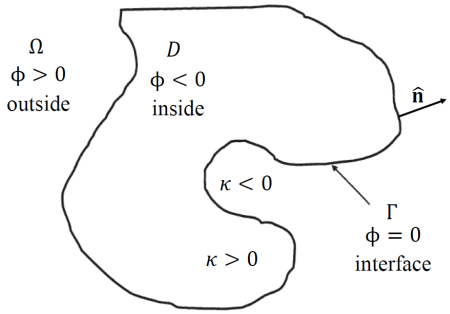

Figure 3.1: *Graphical representation of the level-set function.*

3.5.1 Properties of the level-set function

Some convenient and interesting properties follow from Definition (3.18).

Unit normal

The gradient, $\nabla\phi$, is perpendicular to the iso-contours of ϕ and points in the direction of increasing ϕ (that is, from the material to the void). Let $\mathbf{x}_0$ be a point on the zero isocontour of ϕ, i.e., a point on the interface, then $\nabla\phi(\mathbf{x}_0)$ is a vector that points in the same direction as the local unit normal vector, $\hat{\mathbf{n}}$, to the interface. Thus, we can express this normal vector in terms of the level-set function for points on the interface.

$$\hat{\mathbf{n}}(\mathbf{x}) = \frac{\nabla\phi(\mathbf{x})}{\|\nabla\phi(\mathbf{x})\|_2}. \tag{3.19}$$

Note that this holds for any interface $\phi = a$ with $a \in \mathbb{R}$.

Mean curvature

When we want to know whether a region is convex or concave, we take a look at the mean curvature of the interface, that is, the divergence of the normal vector,

$$\kappa := \frac{1}{d-1} \nabla \cdot \hat{\mathbf{n}}, \tag{3.20}$$

where d is the spatial dimension. Note that we can express the mean curvature in terms of the level-set function as well by using the expression of the unit normal vector in Equation (3.19). Substituting this expression into the definition of the mean curvature, Definition (3.20), results in

$$\kappa(\mathbf{x}) = \frac{1}{d-1} \nabla \cdot \left(\frac{\nabla \phi(\mathbf{x})}{\|\nabla \phi(\mathbf{x})\|_2} \right). \tag{3.21}$$

So, for convex regions we have $\kappa > 0$, for concave regions $\kappa < 0$ and for a plane $\kappa = 0$.

Volume and surface integrals

Using the Heaviside function, Dirac delta function and a level-set function one can compose a *volume integral* (area or length integral in $\mathbb{R}^2$ or $\mathbb{R}$, respectively) and *surface integral* (line or point integral in $\mathbb{R}^2$ or $\mathbb{R}$, respectively) over the entire reference domain Ω.
The Heaviside function (named after Oliver Heaviside) is defined as follows using the (one-dimensional) variable ϕ:

$$H(\phi) := \begin{cases} 1 & \text{if } \phi > 0, \\ 0 & \text{if } \phi \leq 0. \end{cases} \tag{3.22}$$

For convenience purposes we define the Dirac delta function (named after Paul Dirac) as the derivative of the Heaviside function

$$\delta(\phi) := H'(\phi). \tag{3.23}$$

As the level-set function is place-dependent, the volume integral of a function $f(\mathbf{x})$ over the interior D is defined as

$$\int_D f(\mathbf{x}) \, \mathrm{d}\Omega := \int_\Omega f(\mathbf{x}) \left(1 - H(\phi(\mathbf{x}))\right) \, \mathrm{d}\Omega. \tag{3.24}$$

Before we move on to the surface integral, we have to show some equalities. Osher and Fedkiw [17] state that the directional derivative of the Heaviside function in the normal direction is a Dirac delta function which depends on the multidimensional variable $\mathbf{x}$

$$\tilde{\delta}(\mathbf{x}) := \nabla H(\phi(\mathbf{x})) \cdot \hat{\mathbf{n}}. \tag{3.25}$$

It is important to remark that this definition differs from the definition used by physicists: $\hat{\delta}(\mathbf{x}) := \delta(x_1) \cdots \delta(x_d)$.

Due to how the level-set function is defined, the function $\tilde{\delta}(\mathbf{x})$ is only non-zero on the interface Γ. With this definition of the Dirac delta function the surface integral of a function $f(\mathbf{x})$ over the boundary Γ is defined as

$$\int_{\Gamma} f(\mathbf{x}) \, \mathrm{d}\Gamma := \int_{\Omega} f(\mathbf{x}) \tilde{\delta}(\mathbf{x}) \, \mathrm{d}\Omega. \tag{3.26}$$

Notice how we go from a boundary integral to an integral over the entire reference domain.
In order for us to implement the level-set function into this surface integral we rewrite Definition (3.25) using the chain rule.

$$\begin{aligned}
\tilde{\delta}(\mathbf{x}) &= \nabla H(\phi(\mathbf{x})) \cdot \hat{\mathbf{n}} \\
&= H'(\phi(\mathbf{x})) \nabla \phi(\mathbf{x}) \cdot \frac{\nabla \phi(\mathbf{x})}{\|\nabla \phi(\mathbf{x})\|_2} \\
&= H'(\phi(\mathbf{x})) \frac{\|\nabla \phi(\mathbf{x})\|_2^2}{\|\nabla \phi(\mathbf{x})\|_2} = H'(\phi(\mathbf{x})) \|\nabla \phi(\mathbf{x})\|_2.
\end{aligned}$$

Substituting Definition (3.23) into the last line gives

$$\tilde{\delta}(\mathbf{x}) = \delta(\phi(\mathbf{x})) \|\nabla \phi(\mathbf{x})\|_2. \tag{3.27}$$

By substituting Equation (3.27) into the surface integral, Definition (3.26), we get

$$\int_{\Gamma} f(\mathbf{x}) \, \mathrm{d}\Gamma = \int_{\Omega} f(\mathbf{x}) \delta(\phi(\mathbf{x})) \|\nabla \phi(\mathbf{x})\|_2 \, \mathrm{d}\Omega. \tag{3.28}$$

The reason we rather use Equations (3.24) and (3.28) is to avoid identifying the interior, exterior and boundary regions for the calculation of the integrals. Instead, both integrals are taken over the entire reference domain Ω.

3.6 Implementing the level-set method

Finally, we have the knowledge to implement the level-set method into the minimum compliance problem, Problem (3.13), and fundamental eigenfrequency maximisation problem, Problem (3.17). From the definitions of the volume integral, Definition (3.24), and surface integral, Definition (3.28), we know how to implement the level-function into the integrals of both problems.

3.6.1 Level-set embedded minimum compliance problem

Combining all this together results in the level-set embedded minimum compliance problem

$$\begin{cases} \min\limits_{\phi} & \tilde{a}(\mathbf{u},\mathbf{u},\phi) \\ \text{s.t.} & \tilde{a}(\mathbf{u},\mathbf{v},\phi) = \tilde{l}(\mathbf{v},\phi) \quad \forall \mathbf{v} \in U_0, \\ & \mathbf{u}\big|_{\Gamma_{\mathrm{D}}} = \mathbf{u}_0, \\ & \phi\big|_{A} = \phi_0, \\ & \tilde{V}(\phi) \leq V_{\max} \int\limits_{\Omega} 1 \,\mathrm{d}\Omega, \end{cases} \tag{3.29}$$

where

$$\tilde{a}(\mathbf{u},\mathbf{v},\phi) := \int\limits_{\Omega} E_{ijkl}\varepsilon_{kl}(\mathbf{u})\varepsilon_{ij}(\mathbf{v})(1-H(\phi)) \,\mathrm{d}\Omega, \tag{3.30}$$

$$\tilde{l}(\mathbf{u},\phi) := \int\limits_{\Omega} (\mathbf{f}\cdot\mathbf{u})(1-H(\phi)) \,\mathrm{d}\Omega + \int\limits_{\Omega} (\mathbf{t}\cdot\mathbf{u})\delta(\phi)\|\nabla\phi\|_2 \,\mathrm{d}\Omega, \tag{3.31}$$

$$\tilde{V}(\phi) := \int\limits_{\Omega} (1-H(\phi)) \,\mathrm{d}\Omega. \tag{3.32}$$

Note that we no longer minimise over the design domain but over the level-set function. That is, because the level-set function describes the design domain. By the same token, we also have a Dirichlet 'boundary' condition for the level-set function on the domain A.

3.6.2 Level-set embedded fundamental eigenfrequency maximisation problem

In the same way we derive the level-set embedded fundamental eigenfrequency maximisation problem

$$\begin{cases} \max\limits_{\phi} & \omega_1^2 \\ \text{s.t.} & \tilde{a}(\mathbf{u}^{(1)},\mathbf{v},\phi) = \omega_1^2 \tilde{b}\left(\mathbf{u}^{(1)},\mathbf{v},\phi\right), \quad \forall \mathbf{v} \in U_0, \\ & \mathbf{u}\big|_{\Gamma_{\mathrm{D}}} = \mathbf{u}_0, \\ & \phi\big|_{A} = \phi_0, \\ & \tilde{V}(\phi) \leq V_{\max} \int\limits_{\Omega} 1 \,\mathrm{d}\Omega, \end{cases} \tag{3.33}$$

where

$$\tilde{b}(\mathbf{u},\mathbf{v},\phi) := \int\limits_{\Omega} \rho(\mathbf{u}\cdot\mathbf{v})(1-H(\phi)) \,\mathrm{d}\Omega. \tag{3.34}$$

Unlike in Definition (3.16), no literature has yet been encounter in which the fundamental eigenfrequency is expressed in terms of the level-set function. We should, however, expect that it is

$$\omega_1^2 = \min_{\mathbf{v}\in U_0 \wedge \mathbf{v}\neq\mathbf{0}} \frac{\tilde{a}(\mathbf{v},\mathbf{v},\phi)}{\tilde{b}(\mathbf{v},\mathbf{v},\phi)}.$$

The next step is choosing methods to solve Problems (3.29) and (3.33). Yet, that is out of the scope of this literature report and left to the final part of the research.

CHAPTER 4

BENCHMARK PROBLEMS

This chapter studies the three benchmarks which will be used in the final report of the thesis to test our level-set based topology optimisation algorithm for the minimum compliance problem. For now, it is there to show the results of another topology optimisation algorithm. Later, these results will serve as benchmarks to compare the results of the level-set approach to.
Benchmarks regarding eigenvalue optimisation are absent, as comprehensive research of this subject has yet to be done. We start this chapter with a brief description of the comparative algorithm.

4.1 Comparative topology optimisation method

The topology optimisation method used for the minimum compliance problem has a few important elements worth mentioning. It uses a density approach known as SIMP (Simple Isotropic Material with Penalisation). It forces the continuous (which is a result of this approach) design variables towards a solid or void solution. Our algorithm has a penalisation factor of $p = 3$. For more information about SIMP see [31], [30] and [8]. The well-known finite-element method (FEM) is used for the discretisation and utilises rectangular elements. Moreover, a Helmholtz filter is used to prevent the checkerboard paterns. The iterative updating is done by the optimality criteria method (OC). The volume constraint is $V_{\max} = 0.4$ and the maximum number of iterations is 50. The stopping criterium could be either one of the following two: the relative change of the objective function is below 10^{-4} or the infinity norm of the solution is below 10^{-2}.

4.2 MBB beam

The Messerschmitt-Bölkow-Blohm (MBB) beam is a well-known standard benchmark problem in the field of topology optimisation (see [29] and [16]). It consists of a

beam for which the bottom left and right points are fixed. So, these two points have homogeneous Dirichlet conditions in the horizontal and vertical direction. On the middle top point a force is exerted as shown in Figure 4.1.

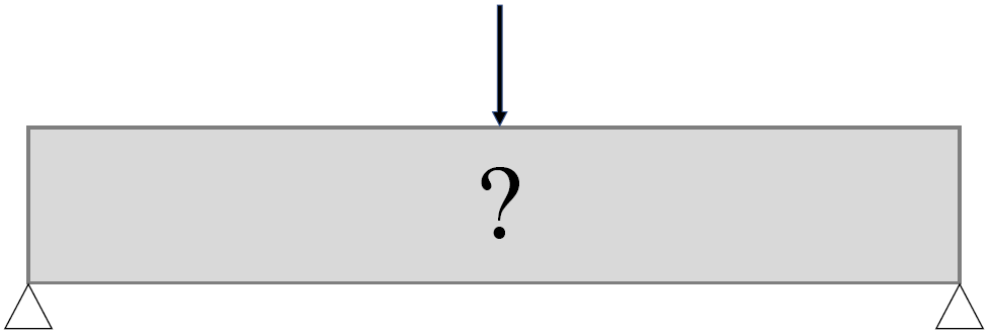

Figure 4.1: *Reference domain of the MBB beam and the boundary conditions.*

Due to symmetry, we merely have to model half of the design. In that case we set the horizontal displacement in the middle of the beam to zero (homogeneous Dirichlet condition). This results in a smaller reference domain, which is computationally more efficient (see Figure 4.2). The rest of the boundary, except the bottom right point, has a homogeneous Neumann condition. For results in other literature see the 2007 paper [28] of Sigmund and 2010 paper [35] of Takewaza et al. (the latter refers to it as a bridge).

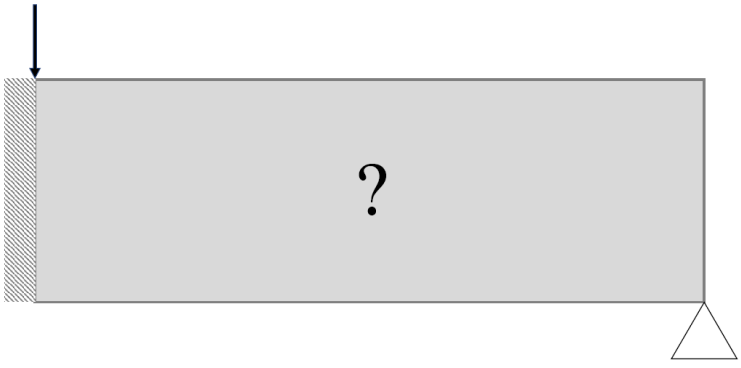

Figure 4.2: *Reference domain of the right-hand side of the MBB beam and the boundary conditions.*

For our MBB beam benchmark problem we consider a length to height ratio of 6:1 (entire beam).

4.2.1 Numerical example MBB beam

For this numerical example 60 elements in the x direction and 20 in the y direction were used. In Figure 4.3 we see three stages of the topology optimisation process of the right-hand side of the MBB beam. Note how the fixed point in the bottom right corner has a different colour than the rest of the initial design (zero iterations). A substantial part of the final structure is already visible after 7 iteration. After 50 iteration there is not yet convergence, as some parts are still green. It should be expected that convergence would be reached if more iterations were allowed.

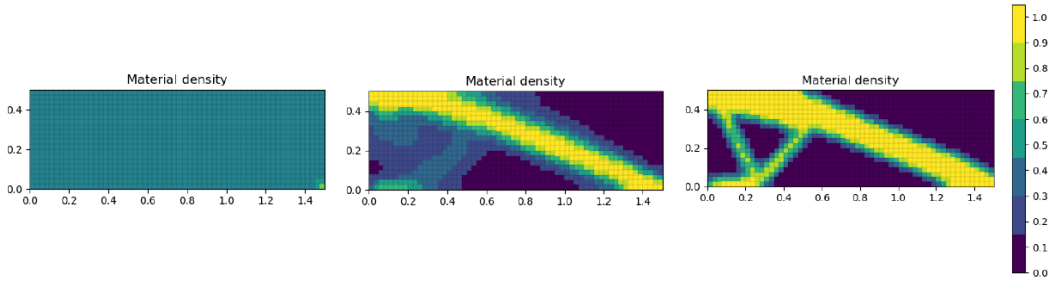

Figure 4.3: *From left to right: 0, 7 and 50 iterations of the MBB beam.*

4.3 Cantilever

If one benchmark problem is required to be present, then it must be the cantilever benchmark problem. In all fields of topology optimisation it is used, as it is a quite simple to implement and solve problem. Some examples of the cantilever in literature are found in [34], [35] and [4].
The cantilever is a rectangle of which the left edge is fixed (as if to a wall). So, we have homogeneous Dirichlet conditions on the entire left-hand side of the rectangle. The other edges of the rectangle have homogeneous Neumann conditions. Furthermore, there is a concentrated force vertically loaded at the centre point of the right-hand side (see figure 4.4). We examine a cantilever with a 2:1 length to height ratio.

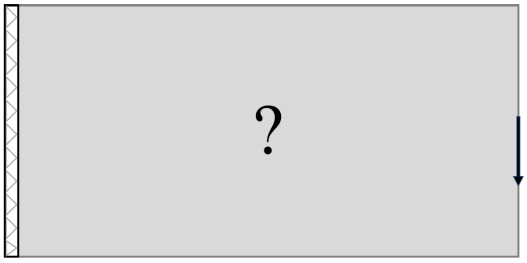

Figure 4.4: *Reference domain of the cantilever and the boundary conditions.*

4.3.1 Numerical example cantilever

For this numerical example 50 elements in the x direction and 25 in the y direction were used. In Figure 4.5 we see three stages of the topology optimisation process of the cantilever. The material constraint of predefined material at the left-hand side is visible in the initial design. It is interesting to see how the material density of this part of the structure decreases, but is still above 0.5. This is the results of the filter. Similar to the MBB beam, the optimal design of the cantilever is becoming plainly noticeable.

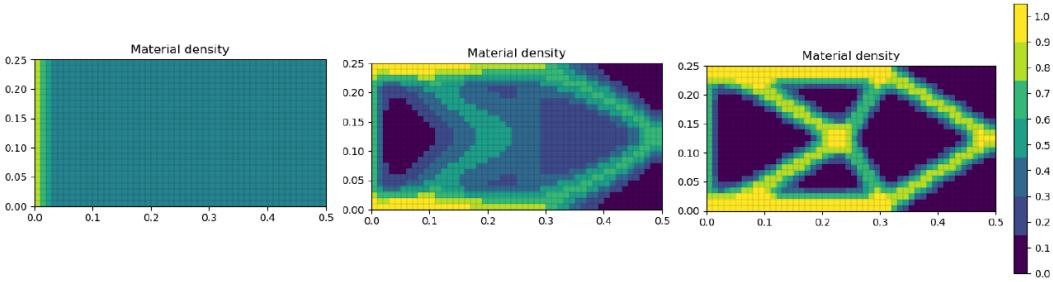

Figure 4.5: *From left to right: 0, 7 and 50 iterations of the cantilever.*

4.4 Inverter

The inverter is to a certain extend different from the MBB beam and cantilever. While the first two benchmark problems have the objective of minimising the compliance, in the inverter problem the objective is to minimise the displacement in a certain point in one direction. On account of this, the inverter benchmark will be dismissed as a compliant mechanism problem and treated as a minimum compliance problem. We do this because of two reasons. First, a compliant mechanism problem would mean a third problem, besides the minimum compliance and eigenfrequency maximisation problems. That would be outside the scope of this thesis. Second, treating it as a minimum compliance problem means that we have three benchmarks. This contributes to a more general applicability of the model and method of solving. It has yet to be decided if all three minimum compliance benchmark problems will be used for the eigenvalue topology optimisation as well. Nonetheless, a short description of the original inverter problem will be provided. The inverter is a "force or displacement-inverting mechanism and is used to change the direction of actuating displacement or force" according to Veguería et al. [38]. The reference domain is a square where the left-hand side top and bottom corners are fixed (homogeneous Dirichlet). A force is exerted on the middle of the same side in the horizontal direction. This force can point to the left of or to the right. A displacement occurs on the right-hand side in the middle of the square and is directed in the opposite direction (see Figure 4.6). This point can only be displaced in the horizontal direction. So, we have a homogeneous Dirichlet condition for the vertical component of this point.
Like the MBB beam, the inverter also has a symmetry property and is illustrated in

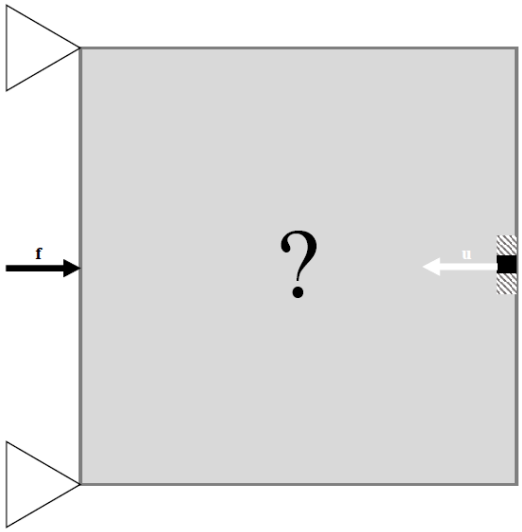

Figure 4.6: *Reference domain of the inverter and the boundary conditions.*

Figure 4.7.
In the setting of minimum compliance we do not alter the physical model of the inverter. The difference is the objective, which is now finding the optimal design wherefore the compliance is minimal.

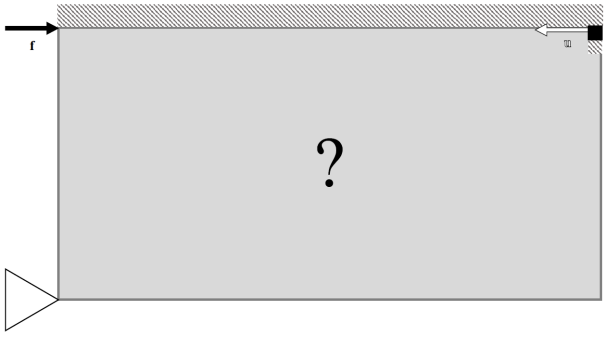

Figure 4.7: *Reference domain of the right-hand side of the inverter and the boundary conditions.*

4.4.1 Numerical example inverter

This numerical example is particularly fascinating as shows one of the numerical problems of the model of the inverter. In Figure 4.8 we see four iterations of inverter with 50 elements in the x direction and in the y direction. After 19 iterations we must conclude that the design is not optimal as it is not path connected. The point in the

top right corner is not connected to the big yellow structure on the left. The initial design as well as the first and second iterations are also depicted in Figure 4.8. After one iteration there are no problems. After the second iteration, however, we see that a structure on the left is forming and is 'disconnecting' from the point in the top right corner. This is could be due to the strong local minimum Sigmund and Maute mention in their review article [30]. It is, however, more likely that this is simply the optimal design, as the used algorithm does not guarantee 'path connectedness'. In this regard, the inverter is not suitable as a minimum compliance problem.

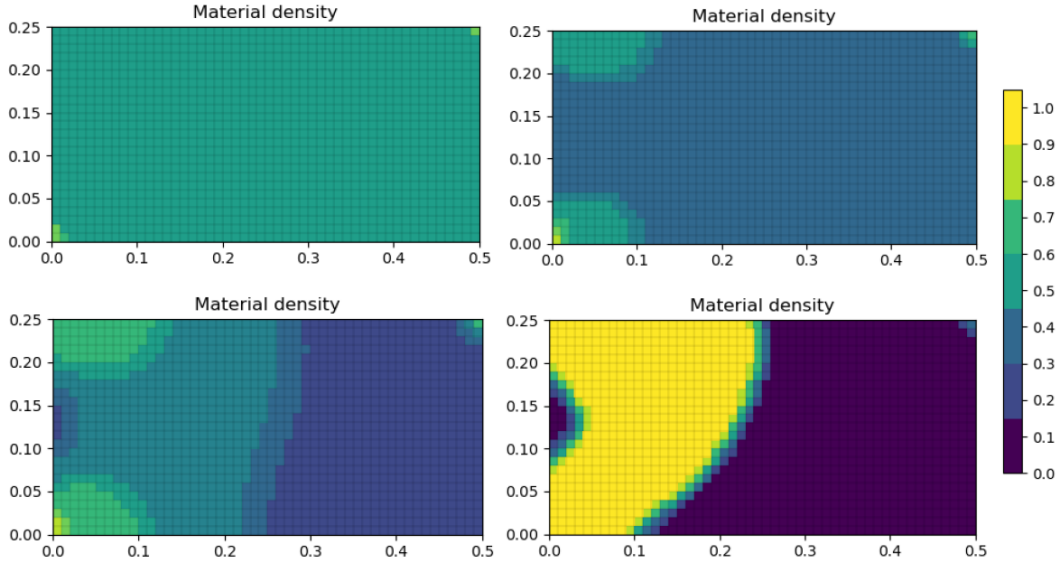

Figure 4.8: *Top left 0, top right 1, bottom left 2 and bottom right 19 iterations of the inverter.*

CHAPTER 5

CONCLUSIVE SUMMARY

After some important clarifications in Chapter 2, the minimum compliance problem was derived. This was done with the use of a weak form (principle of virtual work) acquired from the principle of minimum potential energy. Basic quantities and laws of linear elasticity were introduced to give this report an important foundation in the context of physics. Unlike the minimum compliance problem, the fundamental eigenfrequency maximisation problem was merely put forward without any derivation. During the literature research no derivation of this eigenfrequency problem has been encounter yet. This is one of the objectives of the thesis and might be achieved by more thorough literature research and by asking professors of other departments (e.g. mathematical physics) for advice.
Then the level-set method was introduced as a topology optimisation approach and the level-set function was incorporated in both problems. The next step of the the thesis is solving the level-set embedded minimum compliance problem. In light of this the convected level-set method approach of Yaji et al. [39] is very suitable. They use a sinus filter to obtain a smooth truncation away from the structural boundaries and apply a convected level-set method in order to bypass the need for reinitialisation of the level-set function. After this, we tackle the level-set embedded fundamental eigenfrequency maximisation problem.
Another compelling problem we came across was the absence of 'path connectedness' in the simulation of the inverter problem. This was a result of treating the inverter as a minimum compliance problem. Therefore, the inverter is no longer used as a benchmark in the final report of this thesis.

APPENDIX A

DERIVATION OF THE EQUATION OF MOTION

To derive the equilibrium equation of motion for linear elasticity, we have to alter the right hand side of Equation (3.11).

$$\begin{aligned}\underline{\underline{\sigma}} : \underline{\underline{\varepsilon}}(\mathbf{v}) &= \underline{\underline{\sigma}} : \left[\frac{1}{2}\left(\nabla\mathbf{v} + (\nabla\mathbf{v})^T\right)\right] \\ &= \frac{1}{2}\left[\underline{\underline{\sigma}} : \nabla(\mathbf{v})\right] + \frac{1}{2}\left[\underline{\underline{\sigma}} : (\nabla\mathbf{v})^T\right] \\ &= \frac{1}{2}\left[\underline{\underline{\sigma}} : \nabla(\mathbf{v})\right] + \frac{1}{2}\left[\underline{\underline{\sigma}}^T : (\nabla\mathbf{v})^T\right] \\ &= \frac{1}{2}\left[\underline{\underline{\sigma}} : \nabla(\mathbf{v})\right] + \frac{1}{2}\left[\underline{\underline{\sigma}} : \nabla\mathbf{v}\right] = \underline{\underline{\sigma}} : \nabla(\mathbf{v}).\end{aligned}$$

So we have

$$\underline{\underline{\sigma}} : \underline{\underline{\varepsilon}}(\mathbf{v}) = \underline{\underline{\sigma}} : \nabla(\mathbf{v}).$$

Now Equation (3.11) becomes

$$\int_\Omega \underline{\underline{\sigma}}(\mathbf{u}) : \nabla\mathbf{v} \, \mathrm{d}\Omega = \int_\Omega \mathbf{f}\cdot\mathbf{v} \, \mathrm{d}\Omega + \int_\Gamma \mathbf{t}\cdot\mathbf{v} \, \mathrm{d}\Gamma. \tag{A.1}$$

We introduce the *traction-stress relation* [32] for all $\mathbf{u}$ on the boundary Γ_N:

$$\mathbf{t} = \hat{\mathbf{n}}\cdot\underline{\underline{\sigma}}(\mathbf{u}), \quad t_i = \hat{n}_j\sigma_{ji}(\mathbf{u}), \tag{A.2}$$

where $\hat{\mathbf{n}}$ is the unit normal vector. This gives

$$\mathbf{t}\cdot\mathbf{v} = (\hat{\mathbf{n}}\cdot\underline{\underline{\sigma}}(\mathbf{u}))\cdot\mathbf{v} = \underline{\underline{\sigma}}^T(\mathbf{u})\hat{\mathbf{n}}\cdot\mathbf{v} = \underline{\underline{\sigma}}(\mathbf{u})\mathbf{v}\cdot\hat{\mathbf{n}}.$$

We substitute this into Equation (A.1) and bring the boundary integral to the left hand side.

$$\int_\Omega \underline{\underline{\sigma}}(\mathbf{u}) : \nabla \mathbf{v} \, \mathrm{d}\Omega - \int_\Gamma \underline{\underline{\sigma}}(\mathbf{u})\mathbf{v} \cdot \hat{\mathbf{n}} \, \mathrm{d}\Gamma = \int_\Omega \mathbf{f} \cdot \mathbf{v} \, \mathrm{d}\Omega. \tag{A.3}$$

Now we apply Gauß' divergence theorem [33].

$$\int_\Omega \underline{\underline{\sigma}}(\mathbf{u}) : \nabla \mathbf{v} \, \mathrm{d}\Omega - \int_\Omega \nabla \cdot (\underline{\underline{\sigma}}(\mathbf{u})\mathbf{v}) \, \mathrm{d}\Omega = \int_\Omega \mathbf{f} \cdot \mathbf{v} \, \mathrm{d}\Omega$$

We take a look at the integrand of the second integral on the left hand side and work it out.

$$\begin{aligned}
\nabla \cdot (\underline{\underline{\sigma}}\mathbf{v}) &= \sum_{i,j=1}^{d} \frac{\partial}{\partial x_i}\Big(\sigma_{ij} v_j\Big) \\
&= \sum_{i,j=1}^{d} v_j \frac{\partial \sigma_{ij}}{\partial x_i} + \sum_{i,j=1}^{d} \sigma_{ji} \frac{\partial v_i}{\partial x_j} \\
&= (\nabla \cdot \underline{\underline{\sigma}}^T) \cdot \mathbf{v} + \underline{\underline{\sigma}}^T : \nabla \mathbf{v} = (\nabla \cdot \underline{\underline{\sigma}}) \cdot \mathbf{v} + \underline{\underline{\sigma}} : \nabla \mathbf{v}
\end{aligned}$$

This gives the weak form of the equilibrium equation

$$\int_\Omega \big[\nabla \cdot \underline{\underline{\sigma}}(\mathbf{u}) + \mathbf{f}\big] \cdot \mathbf{v} \, \mathrm{d}\Omega = 0. \tag{A.4}$$

From the Du Bois-Reymond lemma (named after Paul du Bois-Reymond and also know as the Fundamental Lemma of the calculus of variations see [21]) it follows that

$$-\nabla \cdot \underline{\underline{\sigma}}^T(\mathbf{u}) = \mathbf{f}, \quad -\sigma_{ji,j} = f_i. \tag{A.5}$$

Now, together with the traction-stress relation (A.2) and boundary conditions we find that the displacement $\mathbf{u}$ in the field D is the solution of the following boundary value problem:

$$\begin{cases} -\nabla \cdot \underline{\underline{\sigma}}^T(\mathbf{u}) = \mathbf{f}, & \forall \mathbf{u} \in D, \\ \mathbf{u} = \mathbf{u}_0 & \forall \mathbf{u} \in \Gamma_\mathrm{D}, \\ \hat{\mathbf{n}} \cdot \underline{\underline{\sigma}}(\mathbf{u}) = \mathbf{t}, & \forall \mathbf{u} \in \Gamma_\mathrm{N}. \end{cases} \tag{A.6}$$

APPENDIX B

NOMENCLATURE

Notation	Definition	SI unit
$\mathbf{x}$	Place vector	m
$\mathbf{u}$	Displacement vector	m
$\underline{\underline{\varepsilon}}$	Strain-displacement tensor	-
$\underline{\underline{\sigma}}$	Stress tensor	Pa
E	Young's modulus	Pa
ν	Poisson ratio	-
λ	Lamé's first constant	Pa
μ	Lamé's second constant	Pa
E_{ijkl}	Stiffness tensor element	Pa
ω	Eigenfrequency	Hz

BIBLIOGRAPHY

[1] G. Allaire. The Homogenization Method for Topology and Shape Optimization. *Topology Optimization in Structural Mechanics*, 374:101–133, 1997. doi: 10.1007/978-3-7091-2566-3_3.

[2] G. Allaire and F. Jouve. A level-set method for vibration and multiple loads structural optimization. *Computer Methods in Applied Mechanics and Engineering*, 194(30-33 SPEC. ISS.):3269–3290, 2005. ISSN 00457825. doi: 10.1016/j.cma.2004.12.018.

[3] G. Allaire and F. Jouve. Minimum stress optimal design with the level set method. *Engineering Analysis with Boundary Elements*, 32(11):909–918, 2008. ISSN 09557997. doi: 10.1016/j.enganabound.2007.05.007.

[4] G. Allaire, F. Jouve, and A. M. Toader. A level-set method for shape optimization. *Comptes Rendus Mathematique*, 334(12):1125–1130, 2002. ISSN 1631073X. doi: 10.1016/S1631-073X(02)02412-3.

[5] G. Allaire, F. Jouve, and A. M. Toader. *Structural optimization using sensitivity analysis and a level-set method*, volume 194. 2004. ISBN 3316933301. doi: 10.1016/j.jcp.2003.09.032.

[6] S. S. Antman. *Nonlinear Problems of Elasticity*. Springer, New York, second edition, 2005. ISBN 978-0-387-20880-0. doi: https://doi-org.tudelft.idm.oclc.org/10.1007/0-387-27649-1.

[7] M. P. Bendsøe and N. Kikuchi. Generating optimal topologies in structural design using a homogenization method. *Computer Methods in Applied Mechanics and Engineering*, 71(2):197–224, 1988. doi: 10.1016/0045-7825(88)90086-2.

[8] M.P. Bendsøe and O. Sigmund. *Topology optimization: Theory, Methods and Applications*. 2003. ISBN 3540429921. doi: 10.1007/978-3-7091-1309-7_3.

[9] F. De Gournay. Velocity extension for the level-set method and multiple eigenvalues in shape optimization. *SIAM Journal on Control and Optimization*, 45 (1):343–367, 2006. ISSN 03630129. doi: 10.1137/050624108.

[10] J. D. Deaton and R. V. Grandhi. A survey of structural and multidisciplinary continuum topology optimization: Post 2000. *Structural and Multidisciplinary Optimization*, 49(1):1–38, 2014. ISSN 1615147X. doi: 10.1007/s00158-013-0956-z.

[11] V. A. Eremeyev and L. P. Lebedev. Existence of weak solutions in elasticity. *Mathematics and Mechanics of Solids*, 18(2):204–217, 2013. ISSN 10812865. doi: 10.1177/1081286512462187.

[12] T. Lewiński, M. Zhou, and G. I.N. Rozvany. Extended exact least-weight truss layouts-Part II: Unsymmetric cantilevers. *International Journal of Mechanical Sciences*, 36(5):399–419, 1994. ISSN 00207403. doi: 10.1016/0020-7403(94)90044-2.

[13] T. Lewiński, M. Zhou, and G. I.N. Rozvany. Extended exact solutions for least-weight truss layouts-Part I: Cantilever with a horizontal axis of symmetry. *International Journal of Mechanical Sciences*, 36(5):375–398, 1994. ISSN 00207403. doi: 10.1016/0020-7403(94)90043-4.

[14] T. Lewiński, G. I.N. Rozvany, T. Sokół, and K. Bołbotowski. Exact analytical solutions for some popular benchmark problems in topology optimization III: L-shaped domains revisited. *Structural and Multidisciplinary Optimization*, 47 (6):937–942, 2013. ISSN 1615147X. doi: 10.1007/s00158-012-0865-6.

[15] T. Liu, B. Li, S. Wang, and L. Gao. Eigenvalue topology optimization of structures using a parameterized level set method. *Structural and Multidisciplinary Optimization*, 50(4):573–591, 2014. ISSN 16151488. doi: 10.1007/s00158-014-1069-z.

[16] L. Noël, M. Schmidt, C. Messe, J. A. Evans, and K. Maute. Adaptive level set topology optimization using hierarchical B-splines. *Structural and Multidisciplinary Optimization*, 62(4):1669–1699, 2020. doi: 10.1007/s00158-020-02584-6.

[17] S. Osher and R.P. Fedkiw. *Level set methods and dynamic implicit surfaces*. Springer, New York, 2003. ISBN 9781468492514. doi: 10.1007/0-387-22746-6_2.

[18] S. Osher and J. A. Sethian. Fronts propagating with curvature dependent speed: algorithms based on Hamilton-Jacobi formulations. *Journal of Computational Physics*, 148(1):12–49, 1988.

[19] S. J. Osher and F. Santosa. Level Set Methods for Optimization Problems Involving Geometry and Constraints I. Frequencies of a Two-Density Inhomogeneous Drum. *Journal of Computational Physics*, 171(1):272–288, 2001. ISSN 00219991. doi: 10.1006/jcph.2001.6789.

[20] N. L. Pedersen. Maximization of eigenvalues using topology optimization. *Structural and Multidisciplinary Optimization*, 20(1):2–11, 2000. ISSN 1615147X. doi: 10.1007/s001580050130.

[21] F. Rindler. *Calculus of variations*. Springer, 2018. ISBN 9783319776378. doi: 10.1007/978-3-319-77637-8.

[22] G. I. N. Rozvany. Analytical benchmarks in topology optimization - Including probabilistic design. *12th AIAA/ISSMO Multidisciplinary Analysis and Optimization Conference, MAO*, (September):1–11, 2008. doi: 10.2514/6.2008-5941.

[23] G. I. N. Rozvany. On symmetry and non-uniqueness in exact topology optimization. *Structural and Multidisciplinary Optimization*, 43(3):297–317, 2011. ISSN 1615147X. doi: 10.1007/s00158-010-0564-0.

[24] J. J. Rushchitsky. *Nonlinear elastic waves in materials*. Springer, 2014. ISBN 9783319004631. doi: 10.1007/978-3-319-00464-8.

[25] M. H. Sadd. *Elasticity: Theory, applications, and numerics, third edition*. 2014. ISBN 9780124081369. doi: 10.1016/B978-0-12-408136-9.01001-1.

[26] J. A. Sethian and A. Wiegmann. Structural Boundary Design via Level Set and Immersed Interface Methods. *Journal of Computational Physics*, 163(2):489–528, 2000. ISSN 00219991. doi: 10.1006/jcph.2000.6581.

[27] O. Sigmund. On the design of compliant mechanisms using topology optimization. *Mechanics of Structures and Machines*, 25(4):493–524, 1997. ISSN 08905452. doi: 10.1080/08905459708945415.

[28] O. Sigmund. Morphology-based black and white filters for topology optimization. *Structural and Multidisciplinary Optimization*, 33(4-5):401–424, 2007. ISSN 1615147X. doi: 10.1007/s00158-006-0087-x.

[29] O. Sigmund. Manufacturing tolerant topology optimization. *Acta Mechanica Sinica*, 25(2):227–239, 2009. ISSN 05677718. doi: 10.1007/s10409-009-0240-z.

[30] O. Sigmund and K. Maute. Topology optimization approaches: A comparative review. *Structural and Multidisciplinary Optimization*, 48(6):1031–1055, 2013. ISSN 1615147X. doi: 10.1007/s00158-013-0978-6.

[31] O. Sigmund and J. Petersson. Numerical instabilities in topology optimization: A survey on procedures dealing with checkerboards, mesh-dependencies and local minima. *Structural Optimization*, 16(1):68–75, 1998. ISSN 09344373. doi: 10.1007/BF01214002.

[32] W.S. Slaughter and J. Petrolito. *The Linearized Theory of Elasticity*. Springer, 2002. ISBN 9781461266082. doi: 10.1115/1.1497478.

[33] M.R. Spiegel. *Vector Analysis*. Schaum;s Outlines, 2010. doi: 10.1119/1.1933387.

[34] K Suzuki and N Kikuchi. A homogenization method for shape and topology optimization. *Computer Methods in Applied Mechanics and Engineering*, 93(3): 291–318, 1991. ISSN 01608835. doi: 10.1016/0045-7825(91)90245-2.

[35] A. Takezawa, S. Nishiwaki, and M. Kitamura. Shape and topology optimization based on the phase field method and sensitivity analysis. *Journal of Computational Physics*, 229(7):2697–2718, 2010. ISSN 10902716. doi: 10.1016/j.jcp.2009.12.017. URL `http://dx.doi.org/10.1016/j.jcp.2009.12.017`.

[36] L. H. Tenek and I. Hagiwawa. Eigenfrequency maximization of plates by optimization of topology using homogenization and mathematical programming. *Chemical Pharmaceutical Bulletin*, 37(4):667–677, 1994. doi: https://doi.org/10.1299/jsmec1993.37.667.

[37] N. P. Van Dijk, K. Maute, M. Langelaar, and F. Van Keulen. Level-set methods for structural topology optimization: A review. *Structural and Multidisciplinary Optimization*, 48(3):437–472, 2013. ISSN 16151488. doi: 10.1007/s00158-013-0912-y.

[38] E. Veguería, R. Ansola, A. Maturana, and J. Canales. Topology synthesis of compliant mechanisms using an evolutionary method. In *International Conference on Engineering Optimization*, 2008.

[39] K. Yaji, M. Otomori, T. Yamada, K. Izui, S. Nishiwaki, and O. Pironneau. Shape and topology optimization based on the convected level set method. *Structural and Multidisciplinary Optimization*, 54(3):659–672, 2016. ISSN 16151488. doi: 10.1007/s00158-016-1444-z. URL `http://dx.doi.org/10.1007/s00158-016-1444-z`.

[40] T. Yamada, K. Izui, S. Nishiwaki, and A. Takezawa. A topology optimization method based on the level set method incorporating a fictitious interface energy. *Computer Methods in Applied Mechanics and Engineering*, 199(45):2876–2891, 2010. ISSN 00457825. doi: 10.1016/j.cma.2010.05.013. URL `http://dx.doi.org/10.1016/j.cma.2010.05.013`.